

Complex magnetic structure in (LaMnO₃)/(SrMnO₃) superlattices

S. J. May,^{1,*} S. G. E. te Velthuis,¹ M. R. Fitzsimmons,² X. Zhai,³ J. N. Eckstein,³ S. D. Bader,^{1,4} and A. Bhattacharya^{1,4,†}

¹ *Materials Science Division, Argonne National Laboratory, Argonne, IL*

² *Los Alamos National Laboratory, Los Alamos, NM*

³ *Department of Physics, University of Illinois, Urbana-Champaign, IL*

⁴ *Center for Nanoscale Materials, Argonne National Laboratory, Argonne, IL*

(Dated: July 16, 2022)

We present evidence of complex magnetic order in a ferromagnetic (LaMnO₃)_{11.7}/(SrMnO₃)_{4.4} superlattice deposited on SrTiO₃ by ozone-assisted molecular beam epitaxy. Polarized neutron reflectivity (PNR) measurements reveal the presence of a modulated magnetic structure in the superlattice that repeats every bilayer. The magnetic states of the interfaces differ from the non-interfacial LaMnO₃ layers, which exhibit a ferromagnetic moment of $\sim 2.6 \mu_B/\text{Mn}$. An enhanced magnetization is observed at the LaMnO₃/SrMnO₃ (LMO/SMO) interfaces, consistent with interfacial ferromagnetism due to charge delocalization at the LMO/SMO junctions. However, the SMO/LMO interfaces are found to have a reduced ferromagnetic moment. The PNR data does not fit models in which the ferromagnetism is due to either a constant magnetization within the LMO layers or a large magnetization arising symmetrically at the LMO/SMO and SMO/LMO interfaces. Coinciding with the non-uniform magnetic structure is a positive magnetoresistance, which persists up to 2.5 T at low temperatures.

PACS numbers: 75.47.Jn, 61.12.Ha, 75.70.Cn, 75.47.-m

Recent advances in thin film deposition techniques permit the exploration of novel phases emerging at atomically sharp interfaces between dissimilar transition metal oxide compounds.¹ These interfaces can exhibit properties not present in either of the adjoined compounds, such as metallic conductivity between a band insulator (SrTiO₃) and a Mott insulator (LaTiO₃), or ferromagnetism between an antiferromagnet (CaMnO₃) and a paramagnet (CaRuO₃).^{2,3} The manganites, in particular, are excellent candidates in the search for novel interfacial phases due to the wide range of charge, orbital and magnetic ordering phenomena they exhibit.⁴ In bulk form, LaMnO₃ (LMO) is a Mott insulator (Mn^{3+} , $t_{2g}^3 e_g^1$) with *A*-type antiferromagnetic ordering, while SrMnO₃ (SMO) is a band insulator (Mn^{4+} , $t_{2g}^3 e_g^0$) with *G*-type antiferromagnetic ordering. Alloying LMO and SMO yields the mixed-valence ($\text{Mn}^{3+/4+}$) compound, $\text{La}_{1-x}\text{Sr}_x\text{MnO}_3$, which exhibits double-exchange-mediated ferromagnetism for $0.15 < x \leq 0.5$. Similarly, one may expect a ferromagnetic region of one or two unit cells to arise at a LMO/SMO interface due a local mixed-valence state brought about by the transfer of e_g electrons from LMO into SMO.⁵ Investigations of (LMO)_{*k*}/(SMO)_{*j*} superlattices ($0.2 \leq j/(k+j) \leq 0.5$), where *k* and *j* are the number of unit cells in each layer, have examined their macroscopic magnetic and electronic transport properties,^{6,7} structural and chemical profile,⁸ interfacial density of states,^{9,10} and the metal-insulator transition that occurs as the distance between interfaces is increased.¹¹ The collective results of these studies indicate that superlattices comprised of thin bilayers ($k+j \leq 8$) are ferromagnetic metals similar to bulk LSMO compounds, while superlattices with thick bilayers ($k+j \geq 9$) are insulating with reduced values of the

magnetization and Curie temperature (T_C). While the ferromagnetism measured in the latter class of superlattices is often assumed to reside at the interfaces, direct measurements of the magnetic structure have not been reported.

We have investigated the magnetic structure of a [(LMO)_{11.7}/(SMO)_{4.4}]₆ superlattice using polarized neutron reflectivity (PNR) and magnetoresistance (MR) measurements. Fits to the PNR data indicate the presence of an asymmetric interfacial magnetic structure that repeats every bilayer. A positive MR is measured in the superlattice, but is not observed in a magnetically homogeneous $\text{La}_{2/3}\text{Sr}_{1/3}\text{MnO}_3$ film or (LMO)₂/(SMO)₁ superlattice. This suggests that the positive MR arises due to the complex magnetic order present in the (LMO)_{11.7}/(SMO)_{4.4} superlattice.

(LMO)_{2*n*}/(SMO)_{*n*} superlattices and $\text{La}_{2/3}\text{Sr}_{1/3}\text{MnO}_3$ films were deposited on insulating SrTiO₃ substrates using ozone-assisted molecular beam epitaxy. Details of the deposition procedure are reported in Ref. 12. X-ray reflectivity and diffraction measurements were carried out on a Philips XPert diffractometer to determine the composition and *c*-axis lattice parameters of the superlattices. PNR measurements were made using the ASTERIX facility at LANSCE in the Los Alamos National Laboratory. The MR, defined as $MR = [R(H) - R(H = 0)]/R(H = 0)$, was measured with *H* applied in-plane using a Quantum Design Physical Properties Measurement System. A four point probe geometry was employed with the current flowing in-plane and perpendicular to *H*.

The compositions of the superlattices were determined from refinements of x-ray reflectivity data. Thickness fringes and superlattice peaks are visible in the reflectivity data for all samples, indicating high quality interfaces

persisting over macroscopic distances. The x-ray reflectivity data and refinement for the $n = 5$ sample are shown in Fig. 1(a) as a representative example. The presence of a third Bragg peak ($q = 0.3 \text{ \AA}^{-1}$), which should be suppressed if the ratio of LMO to SMO is 2:1, and the suppression of the fourth Bragg peak ($q = 0.4 \text{ \AA}^{-1}$) indicate that the superlattices have excess LMO and are deficient of SMO in deviating from the 2:1 ratio. The best fit to the data yield a composition of $[(\text{LMO})_{11.7}/(\text{SMO})_{4.4}]_6$ with one unit cell of SMO capping the structure.¹³ Out-of-plane lattice parameters of 3.945 and 3.714 \AA were assumed for LMO and SMO, respectively.¹² The crystal structure of a single $(\text{LMO})_{11.7}/(\text{SMO})_{4.4}$ bilayer is depicted in Fig. 1(b). The three other samples used in this study were a $[(\text{LMO})_{10.8}/(\text{SMO})_{4.2}]_6$ superlattice, a $[(\text{LMO})_2/(\text{SMO})_1]_{27}$ superlattice ($n = 1$), and a $\text{La}_{2/3}\text{Sr}_{1/3}\text{MnO}_3$ film (alloy). The superlattices are of comparable thickness, between 32 and 39 nm, while the alloy film is roughly 96 nm thick.

PNR is a well-established technique used to resolve the magnetic depth profiles of heterojunctions and superlattices.¹⁴ The scattering length density profile of the sample, which includes a nuclear and a magnetic contribution, can be extracted from the reflectivity data measured with the neutrons polarized parallel (R^+) and antiparallel (R^-) to the magnetization of the sample. We did not perform polarization analysis, as the magnetization was assumed to be parallel to the in-plane field (0.55 T) applied throughout the measurement.

Figure 1(c) shows the PNR data measured on the $n = 5$ sample at 300 K, well above the Curie temperature of the superlattice ($T_C \approx 180 \text{ K}$). The R^+ and R^- reflections are equal, confirming the lack of ferromagnetism at room temperature. The nuclear potentials of the LMO and SMO layers were obtained by fitting the reflectivity, assuming zero magnetization in the sample. The superlattice was then field-cooled in 0.55 T to 10 K. At these conditions, the sample magnetization ($M = 1.93 \mu_B/\text{Mn}$) is nearly saturated ($M_{\text{sat}} = 2.02 \mu_B/\text{Mn}$). The low temperature PNR data are shown in the inset of Fig. 1(c). A difference is observed between the R^+ and R^- data at 10 K, indicating the sample magnetization is contributing to the scattering potential. Bragg reflections are seen at $q = 0.1$ and 0.2 \AA^{-1} , corresponding to a modulation of the scattering potential. Using the equation $q = 2\pi n/d$, the repeat period of the potential, d , is determined to be 6.26 nm, which is equal to the thickness of each bilayer. As demonstrated by the room temperature measurements, the modulation of the nuclear potential is insufficient to produce the Bragg peaks measured at 10 K. Instead, a modulation of the magnetic potential that is ~ 6 times larger than the difference in the nuclear potentials of SMO and LMO is required to create Bragg peaks of the same magnitude as those observed at 10 K. Thus, the measured Bragg reflections rule out the possibility that the magnetization is constant throughout the superlattice.

Dozens of possible magnetic structures were employed

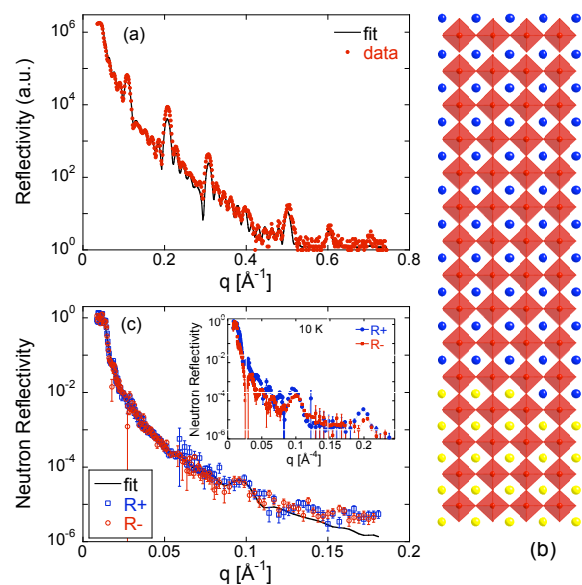


FIG. 1: X-ray reflectivity of $n = 5$ superlattice (a). The solid line shows the fit yielding the composition. The crystal structure of a single bilayer is depicted in (b) with the Sr atoms as blue spheres, La as yellow spheres and MnO_6 octahedra are in red. The PNR measured at 300 K is given in (c) with the solid line showing the fit from which the nuclear scattering length densities of LMO and SMO were determined. For comparison, the PNR measured at 10 K is shown in the inset of (c).

as initial guesses to fit the PNR data using the `co_refine` computer routine.¹⁴ The fitting parameters were restricted to ensure that the local magnetization did not exceed $4 \mu_B/\text{Mn}$ anywhere in the structure. In the fits, all ferromagnetic moments are assumed to be parallel to the in-plane applied field. The magnetization in the surface layers and the SMO layers directly adjacent to the SrTiO_3 substrate was free to differ from the rest of the superlattice. A magnetic structure that has been suggested is one in which ferromagnetism arises symmetrically at the interfaces while the non-interfacial layers of the superlattice are antiferromagnetic.^{5,7} Multiple variations of this scenario were tested by constraining the magnetic scattering length densities to achieve symmetric interfaces, none of which fit the data. In general, the Bragg reflection intensities at $q = 0.1 \text{ \AA}^{-1}$ calculated from profiles with large, symmetric interfacial magnetizations are less than what was measured by roughly an order of magnitude. As an example, Fig. 2(a) shows a fit in which the three LMO unit cells and one SMO unit cell at each interface are ferromagnetic ($\sim 3.3 \mu_B/\text{Mn}$), while the remaining SMO and LMO layers possess reduced ferromagnetic moments, < 0.03 and $1.2 \mu_B/\text{Mn}$, respectively. The resulting fit does not reproduce the data. Poor fits also rule out the possibility that there is a constant magnetization in the LMO layer and no magnetization in the SMO layer, as shown in Fig. 2(b). Note

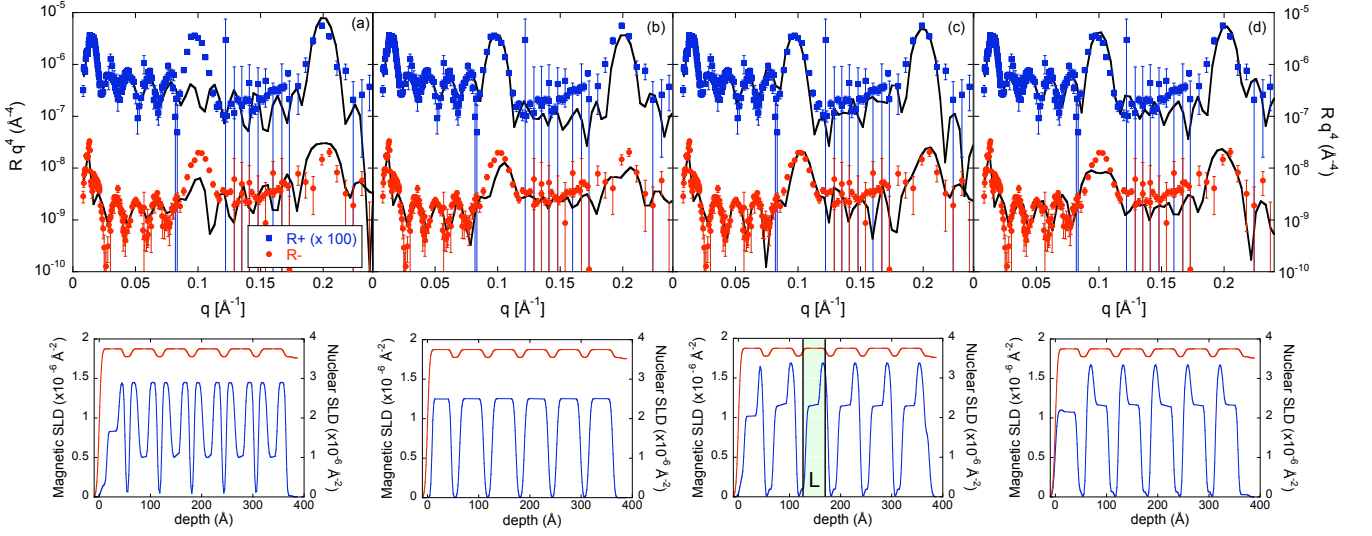


FIG. 2: PNR multiplied by q^4 measured at 10 K. For clarity, the R^+ data has been multiplied by 100. The black lines show fits obtained assuming (a) a large magnetization is present at both LMO/SMO and SMO/LMO interfaces with an equal magnitude, (b) a constant magnetization is present in the LMO layers with a negligible magnetization in the SMO layers, and (c,d) the magnetization is asymmetric about the LMO/SMO and SMO/LMO interfaces. The fit in (c) is the best fit obtained for the PNR data. The corresponding depth profile of the magnetic (blue) and nuclear (red) scattering length densities (SLD) is given below the fit. The higher nuclear SLD corresponds to the LMO layers. For reference, $3 \pm 0.1 \mu_B/\text{Mn}$ corresponds to a magnetic SLD of 1.3×10^{-6} and $1.4 \times 10^{-6} \text{\AA}^{-2}$ in the LMO and SMO, assuming cell volumes of 60.15 and 56.65 \AA^3 , respectively.

the disagreement between the fit and the data at the R^- Bragg reflections.

The best fit, shown in Fig. 2(c), yields a magnetic structure in which enhanced interfacial ferromagnetic moments ($3.8 \mu_B/\text{Mn}$) arise at each LMO/SMO junction, extending over three LMO unit cells. However, a reduced ferromagnetic moment is present at the SMO/LMO interfaces with $< 0.1 \mu_B/\text{Mn}$ in the 6 \AA of LMO at the interface. The non-interfacial LMO layers have a moment of $2.6 \mu_B/\text{Mn}$. In contrast, the non-interfacial SMO layers (one unit cell from the interface) have a negligible magnetization ($< 0.1 \mu_B/\text{Mn}$). The integrated magnetization obtained from the fit is within 6 % of the value measured by SQUID magnetometry.

While a symmetric profile may be expected from purely physical arguments, issues related to materials synthesis can play a role in stabilizing the interfacial ferromagnetic structure. Local strain variations, differences in the morphology of surface terminations between LMO and SMO, or interfacial stoichiometry effects may be the origin of the asymmetric magnetic profile observed in the present study. This asymmetric magnetic profile is an unexpected result that illustrates the need for advanced characterization of interfacial ordering phenomena. PNR is well suited to study interfacial magnetism as it enables the separation of contributions from different interfaces. Figure 2(d) illustrates this point, showing the fit obtained by forcing the enhanced (reduced) ferromagnetic moment to reside at the SMO/LMO (LMO/SMO) interface, opposite to what was determined from the best fit [Fig. 2(c)]. The fit shown in Fig. 2(d) does not repro-

duce the R^- Bragg reflections.

In the same sample ($n = 5$), a positive MR is measured. A unique feature of the positive MR is its presence both as the field is increased from zero and decreased from high fields, as shown in Fig. 3(a). This is in contrast to the positive giant MR or tunnelling MR measured in magnetic trilayers, where the positive MR state is only observed as the magnitude of the field is increased. At fields larger than ~ 2.5 T, the MR becomes negative, presumably due to the colossal MR effect. The positive MR was also observed in the $[(\text{LMO})_{10.8}/(\text{SMO})_{4.2}]_6$ superlattice, confirming that the effect is reproducible. The MR is independent of the angle between the current and applied magnetic field, indicating that the positive MR is not due to the anisotropic MR effect.

Three experimental findings support the assumption that the positive MR results from the complex magnetic structure. First, as shown in Fig. 3(b), the positive MR is not measured in either the $\text{La}_{2/3}\text{Sr}_{1/3}\text{MnO}_3$ alloy film or the $[(\text{LMO})_2/(\text{SMO})_1]_{27}$ superlattice ($n = 1$), which are magnetically homogeneous.^{11,15} Second, the positive MR in the $[(\text{LMO})_{10.8}/(\text{SMO})_{4.2}]_6$ superlattice persists up to ~ 190 K, while the positive MR in the $[(\text{LMO})_{11.7}/(\text{SMO})_{4.4}]_6$ superlattice persists up to ~ 50 K, even though both samples have similar macroscopic T_C values (~ 180 K). This suggests that the strength of the mechanism responsible for the positive MR is dependent on the physical structure. Presumably, the magnetic structure is also dependent on the superlattice structure, specifically the distance between interfaces and the interfacial abruptness. Finally, the positive MR is maximized

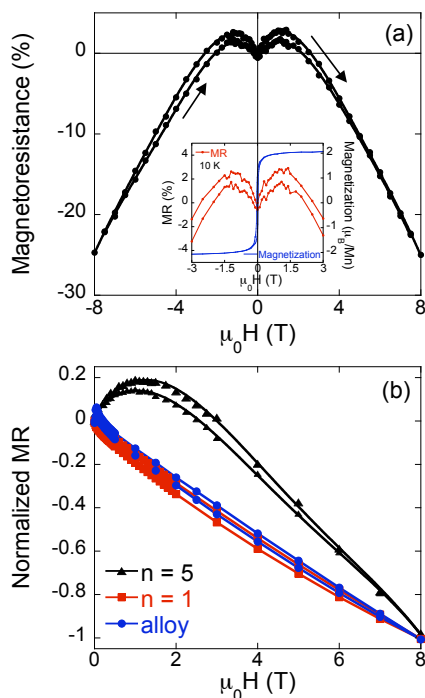


FIG. 3: Magnetoresistance as a function of applied field for the $n = 5$ sample measured at 10 K (a). Shown in the inset of (a) is a comparison of the magnetization and MR. A comparison of the magnetoresistance measured at 6 K in the $n = 5$, $n = 1$, and alloy film is given in (b). The magnetoresistance has been normalized to the MR measured at 8 T.

at fields much larger than the coercive field measured by magnetometry ($\mu_0 H_C \approx 32$ mT at 10 K), as can be seen in the inset of Fig. 3(a), suggesting that the effect is not the result of domain reversals but instead arises from a gradual canting or rearrangement of non-parallel spins within the magnetic structure. This spin rearrangement likely occurs in layers of the superlattice that have a low magnetic moment (the SMO) as the magnitude of the positive MR continues to increase after the ferromagnetism has saturated. However, one would expect a

simple canting process to produce a negative MR as the spins become more aligned with the magnetic field.

While a specific origin cannot be confirmed at this point, one mechanism that produces positive MR in magnetic superlattices can be ruled out. Positive MR is known to arise in antiferromagnetically coupled superlattices and multilayers consisting of ferromagnetic layers with moments oriented antiparallel to one another.^{16,17} However, the PNR and magnetization measurements indicate that the applied field required to ferromagnetically align the bilayers in the $n = 5$ superlattice is less than half the field at which the positive MR is maximized. As an alternative, we speculate that the positive MR arises from a field-induced spin rearrangement at the interfaces between regions of antiferromagnetism and weak ferromagnetism.

In conclusion, we have confirmed the existence of a modulated magnetic structure in ferromagnetic (LaMnO₃)/(SrMnO₃) superlattices. Enhanced interfacial ferromagnetism was observed at each LMO/SMO interface, while the SMO/LMO interfaces have reduced ferromagnetic moments, suggesting that materials synthesis plays a role in stabilizing emergent interfacial phases. We have also identified a positive magnetoresistance coinciding with the non-uniform magnetic structure. These results serve as examples of novel phenomena that can emerge in interfacial complex oxide systems.

We thank Axel Hoffmann for fruitful discussions. Work at Argonne is supported by the U.S. Department of Energy (DOE), Office of Basic Energy Sciences under contract DE-AC02-06CH11357. Work at the University of Illinois at Urbana-Champaign was supported by the DOE, Division of Materials Science under award DEFG02-91-ER45439 through the Frederick Seitz Materials Research Laboratory. This work has benefited from the use of the Lujan Neutron Scattering Center at LANSCE, which is funded by the Department of Energy's Office of Basic Energy Science. Los Alamos National Laboratory is operated by Los Alamos National Security LLC under DOE Contract DE-AC52-06NA25396.

* Electronic address: smay@anl.gov

† Electronic address: anand@anl.gov

- ¹ M. R. Fitzsimmons, S. D. Bader, J. A. Borchers, G. P. Felcher, J. K. Furdyna, A. Hoffmann, J. B. Kortright, I. K. Schuller, T. C. Schulthess, S. K. Sinha, et al., *J. Magn. Mater.* **271**, 103 (2004).
- ² A. Ohtomo, D. A. Muller, J. L. Grazul, and H. Y. Hwang, *Nature* **419**, 378 (2002).
- ³ K. S. Takahashi, M. Kawasaki, and Y. Tokura, *Appl. Phys. Lett.* **79**, 1324 (2001).
- ⁴ M. B. Salamon and M. Jaime, *Rev. Mod. Phys.* **73**, 583 (2001).
- ⁵ C. Lin, S. Okamoto, and A. J. Millis, *Phys. Rev. B* **73**, 041104(R) (2006).

- ⁶ P. A. Salvador, A. M. Haghiri-Gosnet, B. Mercey, M. Hervieu, and B. Raveau, *Appl. Phys. Lett.* **75**, 2638 (1999).
- ⁷ T. Koida, M. Lippmaa, T. Fukumura, K. Itaka, Y. Matsumoto, M. Kawasaki, and H. Koinuma, *Phys. Rev. B* **66**, 144418 (2002).
- ⁸ J. Verbeeck, O. I. Lebedev, G. Van Tendeloo, and B. Mercey, *Phys. Rev. B* **66**, 184426 (2002).
- ⁹ T. Satoh, K. Miyano, Y. Ogimoto, H. Tamaru, and S. Ishihara, *Phys. Rev. B* **72**, 224403 (2005).
- ¹⁰ S. Smadici, P. Abbamonte, A. Bhattacharya, X. Zhai, J. N. Eckstein, J. Zuo, and A. Rusydi, *cond-mat/0705.4501v2*.
- ¹¹ A. Bhattacharya, *et al.*, to be submitted.
- ¹² A. Bhattacharya, X. Zhai, M. Warusawithana, J. N. Eck-

- stein, and S. D. Bader, Appl. Phys. Lett. **90**, 222503 (2007).
- ¹³ The reflectivity represents an average over the $1.4 \times 1.4 \text{ cm}^2$ sample. From the deposition geometry, we expect gradients of up to 5 % in the La/Sr/Mn ratio across the substrate.
- ¹⁴ M. R. Fitzsimmons and C. F. Majkrzak, in *Modern Techniques for Characterizing Magnetic Materials*, edited by Y. Zhu (Springer, New York, 2005), chap. 3, pp. 107–155.
- ¹⁵ J. J. Kavich, J. W. Freeland, *et al.*, to be submitted ($n = 1$ and alloy have the same x-ray magnetic circular dichroism spectrum).
- ¹⁶ I. N. Krivorotov, K. R. Nikolaev, A. Y. Dobin, A. M. Goldman, and E. D. Dahlberg, Phys. Rev. Lett. **86**, 5779 (2001).
- ¹⁷ S. Maekawa and T. Shinjo, eds., *Spin Dependent Transport in Magnetic Nanostructures* (Taylor and Francis, London, 2002).